Int. J. Heat Mass Transfer. Vol. 32, No. 5, pp. 863–871, 1989
Printed in Great Britain

0017–9310/89 $3.00 + 0.00

An effective model for measuring transient natural convective heat flux in vertical parallel plates with a rectangular rib

Y. H. HUNG and W. M. SHIAU
Department of Power Mechanical Engineering, National Tsing Hua University, Hsinchu, Taiwan 30043, R.O.C.

(*Received* 13 *May* 1988 *and in final form* 8 *September* 1988)

Abstract—The total heat input for transient natural convection experiments in vertical parallel plates with a rectangular rib is composed of four kinds of heat-transfer mode—radiative heat loss, conductive heat loss, thermal capacity of the test plate, and convective heat transfer in the test channel. Based on this model for measuring transient heat distributions, a dimensionless transient convective heat flux is defined, and two generalized correlations of transient convective heat flux are proposed—one for the power-on transient period and one for the power-off transient period. In addition, by using these acquired q_c'' distributions with the proposed Nu correlations, transient average Nusselt numbers in the transient power-on and power-off periods have been successfully estimated. Satisfactory comparisons have been made between the transient $\overline{Nu}_L$ predictions and experimental data.

INTRODUCTION

IN A TYPICAL electronic package, printed circuit boards (PCBs) are normally mounted in a card cage to form vertical parallel channels. This geometry lends itself to cooling by natural convection. As we know, packaging constraints and electronic considerations, as well as device or system operating modes, lead to a wide variety of heat dissipation profiles along the channel walls. In many cases of interest, four kinds of thermal wall conditions (i.e. two symmetric isothermal plates, a single isothermal plate and an insulated plate, two symmetric isoflux plates, and a single isoflux plate and an insulated plate) are proposed to yield approximate conditions in the prediction of the thermal performance of such configurations [1, 2].

In practice, identical flat pack electronic components mounted on multilayer PCBs with thin copper strips, copper pads or aluminium heat sink plates are often placed next to one another. When each component dissipates approximately the same amount of power, the heat load will be a uniform isoflux heat profile. If any row of electronic components is considered, the heat dissipation can be evaluated as a uniformly distributed isoflux heating, and this row of electronic components can properly be simulated by a large two-dimensional rib with isoflux heating. Therefore, compared with a smooth isoflux heating plate, a plate mounted with parallel vertical ribs under isoflux heating is a more reasonable representation of the real geometric configuration and the heating condition of PCBs.

Although the effect of S/B, where S is the streamwise pitch between two adjacent ribs (measured centreline to centreline) and B is the rib height, on flow characteristics and heat transfer performance in such configurations is significant, natural convection in vertical parallel plates mounted with an array of ribs under isoflux heating is very complicated. Therefore, as a bridge to this kind of complex problem, it is recognized as useful and valuable to perform a preliminary study of natural convection on a regularly ribbed obstruction mounted on a vertical plate with isoflux heating.

Steady-state natural convection in vertical channels with or without a rectangular rib has been studied extensively in refs. [3–5]. As for transient cases, although transient convective heat transfer parameters such as heat transfer coefficient and Nusselt number are essential in exploring the transient behaviour of thermal systems, no information on transient heat transfer parameters is to be found in the existing literature. For this reason, in the existing thermal analysis computer packages, the steady-state heat transfer parameters are usually chosen and applied to estimate the transient behaviour during a transient period—i.e. a quasi-steady assumption is made for a certain short-time interval in the transient period. However, it is not known whether a transient heat transfer parameter can be considered to be a sequence of steady-state heat transfer coefficients. The transient convective heat dissipation in the test channel is a key parameter for determining the transient heat transfer coefficient and Nusselt number. In order to address the above issue and achieve further understanding about transient heat transfer behaviour, the objectives for the present research are to establish an effective model for measuring transient convective heat flux between vertical parallel plates with a two-dimen-

NOMENCLATURE

B	rib height
C_p	specific heat at constant pressure
g	gravitational acceleration [m s^{-2}]
$\bar{h}$	average heat transfer coefficient [W m^{-2} °C^{-1}]
H	channel spacing
k	thermal conductivity [W m^{-1} °C^{-1}]
L	channel height, defined in Fig. 3
$\overline{Nu}_L$	transient average Nusselt number, $q_c'' L/k(\overline{T_w - T_0})$
Q	heat flow rate [W]
q''	heat flux based on test-surface area [W m^{-2}]
Ra_L^*	modified Rayleigh number, $C_p\rho^2\beta g q_c'' L^4/\mu k^2$
T	temperature [°C]
t	time [min].

Greek symbols

β	thermal expansion coefficient [K^{-1}]
ε	emissivity
μ	dynamic viscosity [kg m^{-1} s^{-1}]
ν	kinematic viscosity, μ/ρ [m^2 s^{-1}]
ρ	density [kg m^{-3}].

Superscript

-	average

Subscripts

b	balsa
c	transient convective value
cs	steady-state convective value
i	internal energy change
k	conduction
L	based on channel length
r	radiation
s	stainless-steel sheet
t	total
w	at test surface
0	at channel inlet or the ambient.

sional rectangular rib, and then to determine whether, in the thermal analysis under transient conditions, it is appropriate to use a steady-state Nusselt number based on the instantaneous value of the Rayleigh number (i.e. the 'quasi-steady' approximation). The relationship between the steady-state Nusselt number and steady-state Rayleigh number was established experimentally in ref. [5]. Transient Nusselt numbers are measured under conditions of varying heat flux. Since the heat flux is varying, so also is the Rayleigh number. Then it is seen whether the transient Nusselt number at a given point in time, which corresponds to a given Rayleigh number, is equal to the steady-state Nusselt number corresponding to that Rayleigh number.

EXPERIMENTAL APPARATUS AND METHODOLOGY

Experimental apparatus

Figure 1 shows the overall experimental assembly, which consists of the entire apparatus and main instruments. The measurements for the present experiments are performed in a low-turbulence open-loop wind tunnel, which is designed to be used for natural, forced and mixed convection tests. The wind tunnel facility is used in a buoyancy-assisting flow condition. As for the test plate in the experiment, its schematic is also shown in Fig. 2. The detailed descriptions for the wind tunnel facility and test plate have been reported in ref. [5].

As previously described in ref. [5], the test plate has one 543 Ω and one 548 Ω resistive element embedded in it for heating, and 78 T-type calibrated thermocouples are glued to it at various locations for temperature measurement. Thus, the local temperature distribution along the test surface, including the extruding element, is accurately measured. The air temperatures at the inlet and outlet of the test channel are each measured by two T-type thermocouples. The temperature differences measured by the thermocouples at the inlet and outlet are consistently small.

Two 0–140 V transformers supply power to the heaters, making the input power changeable. A precision digital multimeter (Omega Model-882) is utilized to calibrate the voltage of each transformer. The

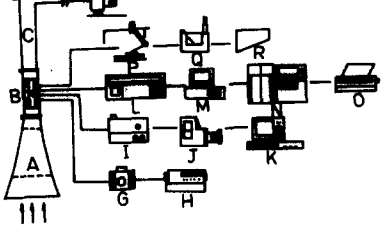

A	nozzle	J	video camera
B	test section	K	video recorder & monitor
C	buffer zone	L	Fluke 2280B data loger
D	cover plate	M	IBM PC-XT Computer
E	flexible tube	N	Apollo computer
F	blower	O	Epson LQ-2500 printer
G	transformer	P	active Pitot-tube supporter
H	digital multimeter	Q	Dwyer microtector
I	Smoke generator	R	Dwyer air meter

FIG. 1. Schematic of experimental air-cooling loop.

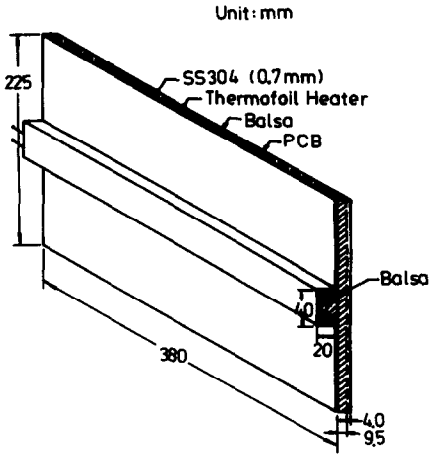

FIG. 2. Schematic of test-plate assembly.

channel spacing between the test plate and an adiabatic shrouding plate is measured by a 30 ± 0.05 cm precision ruler. Both the horizontal and the vertical test plates are calibrated by a water level.

The experiments are controlled and the data are acquired automatically, using a FLUKE-2280B data logging system interfaced to PC-AT based peripherals. The interface between the computer and the test plate is a 2280 Digital Acquisition and Control Unit. The unit has 160 channels of scannable thermally-compensated relays, which are connected to the thermocouples. The data logging system records the local temperature distributions of the test plate during the experiments.

Data reduction

In this study, transient natural convection experiments for vertical parallel plates with a two-dimensional rectangular rib were performed. According to the energy conservation concept, it may be proposed that the total heat generated by the thermofoil heaters, Q_t, is converted into the following four heat-transfer modes at any transient time: (1) radiative heat loss, Q_r; (2) conductive heat loss, Q_k; (3) internal-energy change of the test plate, Q_i; (4) convective heat dissipation in the test channel, Q_c. That is

$$Q_t = Q_r + Q_k + Q_i + Q_c \tag{1}$$

or

$$q_t'' = q_r'' + q_k'' + q_i'' + q_c'' \tag{2}$$

(based on the test-surface area A).

The following are brief descriptions of the models which are proposed to calculate the transient heat distributions.

Estimation of radiative heat loss. During the transient experiments, the average temperature of the test surface (AISI304 surface) is usually higher than the ambient and shrouding wall temperatures. Thus, for radiation exchange, there is a net radiative heat transferred from the test surface to the surroundings.

The radiative heat loss from the test surface to its surroundings is evaluated by using a thermal network analysis. Figure 3(a) presents the numbering and subscript conventions of the analyzing system, and the thermal network of radiative heat transfer relations among the relevant nodes is shown in Fig. 3(b). The shape factor F_{m-n} shown in the figure can be calculated from ref. [7]. In the present study, the radiative heat loss is less than 6.55% of the total input power for all cases.

Estimation of conductive heat loss. To estimate the conductive heat loss from the heater to the fibreglass backplate, a quasi-steady approximation for transient conductive heat loss is assumed. Therefore, a three-dimensional heat conduction analysis with suitable boundary conditions is performed in the present study. The detailed derivation of temperature distributions in an infinite Fourier-series form are shown in ref. [6]; the final expression for the temperature distributions is as follows:

$$T(x, y, z) = T_1(x, y, z) - T_2(x, y, z) \tag{3}$$

where T_1 is the temperature of a surface heated uniformly with a heat flux of q_k'' (Fig. 4(a)), T_2 is the temperature of the centre part heated by a heat flux of $-q_k''$, with the rest of the surface insulated (Fig. 4(b)), and

$$\begin{aligned} T_j(x, y, z) = {} & A_{00}[z - (f + k_b/h)] \\ & + \sum_{n=1}^{\infty} A_{n0} \cos(n\pi x/x_u)[\alpha_n \cosh \alpha_n(z-f) \\ & - (h/k_b) \sinh \alpha_n(z-f)] \\ & + \sum_{m=1}^{\infty} A_{0m} \cos(m\pi y/y_u)[\beta_m \cosh \beta_m(z-f) \\ & - (h/k_b) \sinh \beta_m(z-f)] \\ & + \sum_{n=1}^{\infty} \sum_{m=1}^{\infty} A_{nm} \cos(n\pi x/x_u) \cos(m\pi y/y_u) \\ & \times [\lambda_{nm} \cosh \lambda_{nm}(z-f) - (h/k_b) \\ & \times \sinh \lambda_{nm}(z-f)] \end{aligned} \tag{4}$$

where

$$j = 1 \text{ or } 2$$

$$\alpha_n = n\pi/x_u$$

$$\beta_m = m\pi/y_u$$

$$\lambda_{nm} = (\alpha_n^2 + \beta_m^2)^{1/2}$$

$$A_{00} = -(q_k''/k_b)(c_j/x_u)(d_j/y_u)$$

$$A_{n0} = \frac{2q_k'' \sin(n\pi c_j/x_u)(d_j/y_u)}{n\pi k_b \alpha_n [\alpha_n \sinh(\alpha_n f) + (h/k_b) \cosh(\alpha_n f)]}$$

$$A_{0m} = \frac{2q_k'' \sin(m\pi d_j/y_u)(c_j/x_u)}{m\pi k_b \beta_m [\beta_m \sinh(\beta_m f) + (h/k_b) \cosh(\beta_m f)]}$$

$$A_{nm} = \frac{4q_k'' \sin(n\pi c_j/x_u) \sin(m\pi d_j/y_u)}{mn\pi^2 k_b \lambda_{nm} [\lambda_{nm} \sinh(\lambda_{nm} f) + (h/k_b) \cosh(\lambda_{nm} f)]}$$

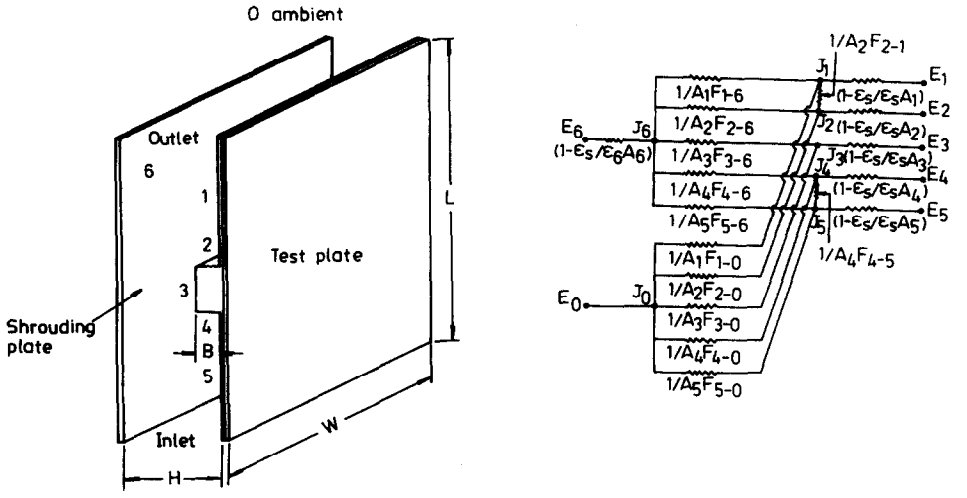

FIG. 3. Radiation heat exchange in test channel.

where c_j represents half of the height of the heated plates and d half the width; f is the thickness of the balsa plate and h an equivalent heat transfer coefficient. In the present experiments, $k_b = 0.04032$ W m^{-1} °C^{-1}, $k_p = 0.175$ W m^{-1} °C^{-1} (the detailed methods of measuring k_b and k_p are described in ref. [6]), $c_1 = x_u = 0.1325$ m, $d_1 = y_u = 0.19$ m, $c_2 = 0.02$ m, $d_2 = 0.19$ m and $f = 0.01$ m.

The theoretical temperature distributions could be solved directly if q_k'' and h were known. However, q_k'' (the conductive heat flux) is unknown, so the solution may not be directly applied in the experiments. On the other hand, the main objective of a detailed analysis is the estimation of this heat flux or conductive heat loss. However, two difficult problems exist in estimating the transient conductive heat loss in the present experiments. One is the determination of the equivalent heat transfer coefficient, h in equation (4). The other is that the real heat flux q_k'' conducted to the balsa wood is an unknown quantity in the experiment. In the analysis, an equivalent heat transfer coefficient is plausibly proposed as the value of k_p/t_p, where k_p and t_p are the conductivity and thickness of the fibreglass board, respectively.

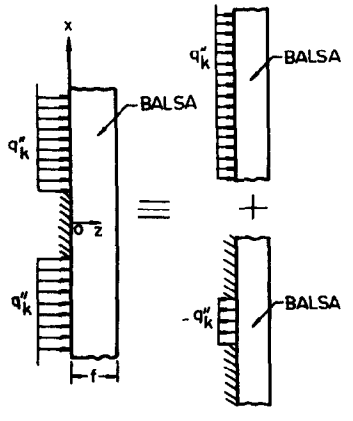

FIG. 4. Superposition technique employed in analysis of conductive heat loss.

Since q_k'' is an implicit parameter, it cannot be calculated directly. Therefore, an iteration method is applied to solve for q_k''; the iteration process will be continued until the local calculated temperatures on both sides of the balsa wood plate approximately equal the experimental data (i.e. within ± 0.005°C).

Estimation of internal energy change. In the present analysis, an experimental method for estimating the internal energy change of the test plate during the transient power-on and power-off periods is postulated. The expression for the internal energy change at a certain time during the transient period is

$$Q_i = Q_s + Q_b \tag{5}$$

or

$$Q_i = \left(\rho C_p V \frac{\Delta \bar{T}}{\Delta t}\bigg|_t\right)_s + \left(\rho C_p V \frac{\Delta \bar{T}}{\Delta t}\bigg|_t\right)_b \tag{6}$$

where Q_s and Q_b represent the internal energy changes in the stainless steel sheet and the balsa wood, respectively, $\rho C_p V$ is the heat capacity of each material, $\bar{T}_s$ the average temperature of the SS304 sheet, $\bar{T}_b$ the average temperature of the balsa wood, and Δt the time interval.

As we know from equation (6), the heat capacities of SS304 sheet and balsa wood used in the experiments should be determined before starting the Q_i calculations. The detailed procedure for the experimental determination of these data can be found in ref. [6]. In addition, the term $\Delta \bar{T}/\Delta t$ in equation (6) may be approximated by $(\bar{T}_{j+1} - \bar{T}_j)/\Delta t$ and calculated with the transient experimental data. Here, $\bar{T}_{j+1}$ is the average temperature of the SS304 sheet or balsa wood at time $t = (j+1)\Delta t$ from the starting time to perform the power-on or power-off transient experiment. Based on the above calculations, the transient internal energy

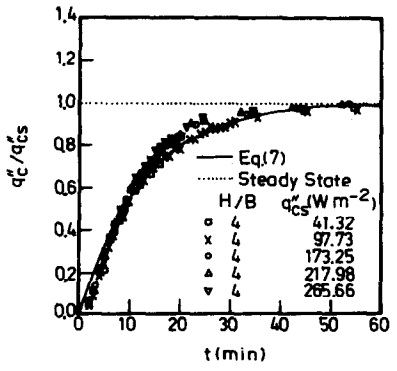

FIG. 5. Effect of steady-state convective heat flux on transient q''_c/q''_{cs} distribution in power-on period.

change of the test plate is estimated to a reasonable accuracy.

Estimation of convective heat flux in the test channel. The determination of experimental transient heat transfer coefficients and Nusselt numbers is strongly dependent on transient convective heat flux in the test channel—therefore the transient convective heat flux requires a precise data reduction in the present experiments. Based on energy conservation, the convective heat flux in the test channel, q''_c, is precisely obtained from equation (1).

Uncertainty analysis

A standard single-sample uncertainty analysis proposed by Kline and McClintock [8] is applied to the experimental data reduction. Thus, temperature measurements in the present experiments are accurate to $\pm 0.2°C$; the uncertainty associated with power input q''_t is determined to be 0.25%, and those of Ra^* and $\overline{Nu}$ in the ranges of the parameters studied (i.e. H/B = 2–8 and q''_{cs} = 41.32–269.35 W m^{-2}) are generally within 6.24 and 4.54%, respectively, except in the cases with very small H and q''_c values in the beginning of the power-on transient period or at the end of the power-off transient period.

EXPERIMENTAL RESULTS AND DISCUSSION

The parameters studied in a series of experiments are channel spacings between 4 and 16 cm (i.e. H/B = 2–8), and steady-state convective heat fluxes ranging from 41.32 to 269.35 W m^{-2}. Twenty data sets with various channel spacings and convective heat fluxes are presented in the experiments. The cases with H = 16 cm (i.e. H/B = 8) can reasonably be considered as the same as the isolated-plate cases in natural convection.

From temperature measurements, the maximum deviations of the local spanwise temperature measurements in three columns of the test surface for all transient experiments are less than 5.6%. Therefore, the two-dimensionality of all experimental results is assured in the power-on and power-off periods.

Before the experimental results in the steady-state condition are displayed, it is necessary to choose the steady state of each experiment. Usually, the steady-state condition is considered to be achieved when the q''_c variation with time is less than 1.0% of the previous q''_c value in each experiment. In general, the steady-state condition will be achieved about 150–180 min after the power is switched on.

Power-on transient period

Figures 5 and 6 show the variation of transient convective heat flux in the test channel with steady-state convective heat flux and channel spacing, respectively. Based on the results shown in the figures, transient convective heat flux at a certain time may be nondimensionalized by the convective heat flux in the steady state of each experiment, and a generalized correlation in an exponential form is then proposed:

$$\frac{q''_c}{q''_{cs}} = 1 - e^{-0.08t} \tag{7}$$

where q''_c is the net heat flux convected to air in the channel at time t in the power-on transient period, q''_{cs} is the steady-state heat flux convected to the air in the channel for each experiment and t the time elapsed since the power was on, expressed in minutes.

Figures 7 and 8 present the variation of average

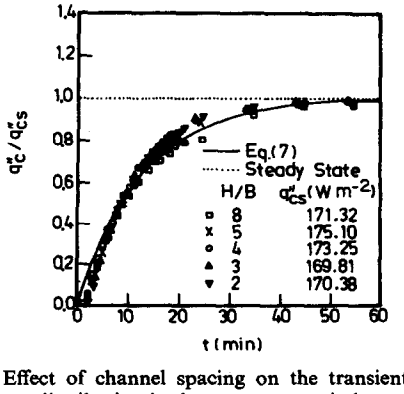

FIG. 6. Effect of channel spacing on the transient q''_c/q''_{cs} distribution in the power-on period

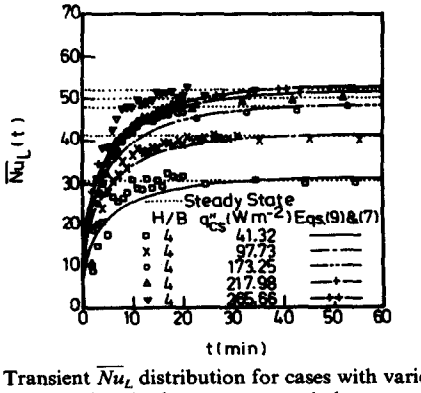

FIG. 7. Transient $\overline{Nu}_L$ distribution for cases with various q''_{cs} values in the power-on period.

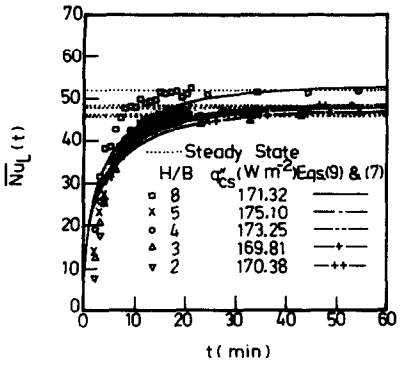

FIG. 8. Transient $\overline{Nu}_L$ distribution for cases with various H/B values in the power-on period.

Nusselt numbers in the power-on transient period with q''_{cs} and H/B, respectively. One inference to be drawn from these figures is that the transient average Nusselt number increases with increasing q''_{cs}. Another important inference is that the channel spacing in the present experiments has no effect on average Nusselt number at any time in the transient period. This surprising result can be demonstrated through flow visualization and experimental measurements—even in the experiments with the narrowest channel spacing, i.e. $H = 4.0$ cm or $H/B = 2$, the boundary layer produced along the test surface is so thin that there is no interaction between the insulated shrouding plate and the boundary layer. Therefore, the channel spacings studied in the present experiments have no effect on heat transfer behaviour.

Figure 9 shows the relationships between the average Nusselt numbers and the modified Rayleigh numbers for all experimental steady-state results, as discussed in ref. [5]. The $\overline{Nu}_L$ correlation derived from ref. [3] and illustrated to be applicable only in the experiments with low convective heat flux (say $Ra^*_L < 10^8$) is also shown in the figure. This correlation can be expressed as

$$\overline{Nu}_L = 0.649 Ra^{*1/5}_L. \quad (8)$$

When the convective heat flux increases, the turbulence originating in the downstream region of the rib becomes stronger. Thus, a new asymptotic limit

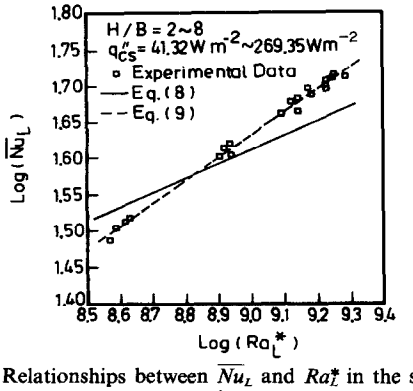

FIG. 9. Relationships between $\overline{Nu}_L$ and Ra^*_L in the steady-state experiments.

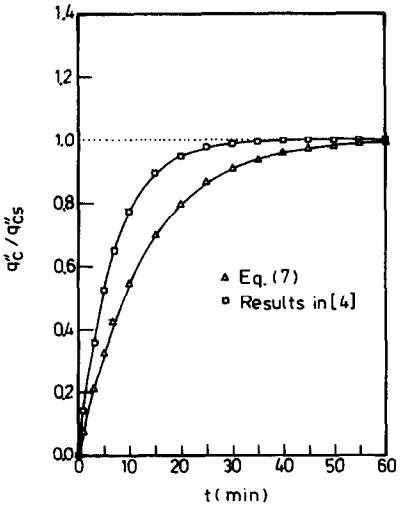

FIG. 10. Comparison of transient q''_c/q''_{cs} distributions between cases with and without a rib in the power-on period.

with a 0.316 power dependence (a value between 1/5 and 1/3) of the average Nusselt number on the modified Rayleigh number is proposed as follows:

$$\overline{Nu}_L = 0.0617 Ra^{*0.316}_L \quad (9)$$

where

$$\overline{Nu}_L = q''_{cs} L / k(\overline{T_w - T_0})$$

and

$$Ra^*_L = C_p \rho^2 \beta g q''_{cs} L^4 / \mu k^2.$$

Both correlations are plotted in Fig. 9 for comparison with experimental results. All thermophysical properties appearing in $\overline{Nu}_L$ and Ra^*_L are evaluated at the film temperature, i.e. $0.5(\bar{T}_w + T_0)$. In the experimental Ra^*_L ranges between 3.75×10^8 and 1.93×10^9, the average deviation of the predictions obtained from equation (8) compared to the present experimental data is 7.45%, with a maximum deviation of 11.59%; whereas the average deviation of the predictions obtained from equation (9) from the experimental data is 1.20%, with a maximum deviation of 3.43%.

If the transient $\overline{Nu}_L$ distributions may be considered as a superposition of a series of quasi-steady states, then the distributions will be calculated by using equation (9) with transient q''_c distributions proposed in equation (7); all thermophysical properties appearing in $\overline{Nu}_L$ and Ra^*_L are evaluated at the transient film temperature, i.e. $0.5(\bar{T}_{wt} + T_0)$. Comparisons between the predicted transient $\overline{Nu}_L$ distributions and the present experimental data are also made, and are shown in Figs. 7 and 8. A satisfactory trend is obtained in the present study.

As compared with the transient q''_c/q''_{cs} distribution for a smooth channel without a rib, which was presented by Perng [9], it is plausibly found that the time needed to reach the steady-state conditions for the present cases is usually longer, because of the existence of the ribbed obstruction (Fig. 10).

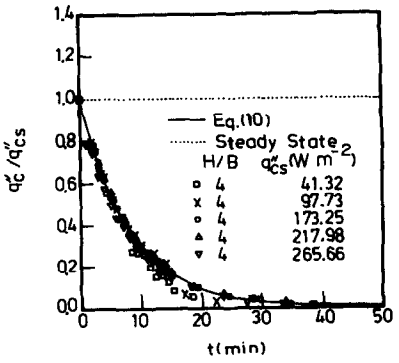

FIG. 11. Effect of steady-state convective heat flux on the transient q_c''/q_{cs}'' distribution in the power-off period.

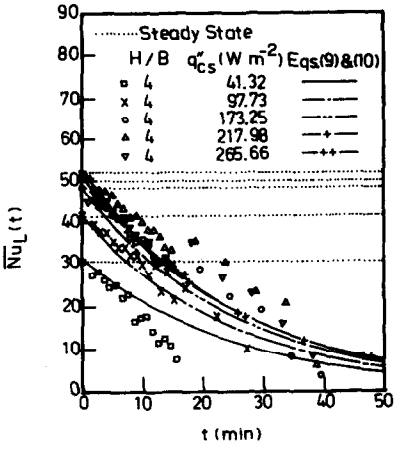

FIG. 13. Transient $\overline{Nu}_L$ distribution for cases with various q_{cs}'' values in the power-off period.

Power-off period

In the present experiments, the steady-state condition will be achieved about 60 min after the power is turned on, and is then maintained for 2 h to perform the steady-state experiments. After completing the steady-state measurements, the power-off transient period will start once the power is turned off.

As mentioned in connection with the power-on transient period, a dimensionless transient convective heat flux of q_c''/q_{cs}'' is also defined in the power-off transient period. Thus, Figs. 11 and 12 show, respectively, the q_{cs}'' and H effects on the transient q_c''/q_{cs}'' distribution. Based on the present experimental data, a similar generalized q_c''/q_{cs}'' correlation is proposed as follows:

$$\frac{q_c''}{q_{cs}''} = e^{-0.12t} \tag{10}$$

where q_c' is the transient convective heat flux from the test surface in the power-off transient period, q_{cs}'' the convective heat flux in the steady-state condition of each experiment and t the elapsed time in the power-off transient period (min).

If the transient $\overline{Nu}_L$ distributions in the power-off period may also be considered as superpositions of a series of quasi-steady states, then the distributions will be calculated by using equation (9) with the transient q_c'' distributions proposed in equation (10); all thermophysical properties appearing in $\overline{Nu}_L$ and Ra_L^* are evaluated at the transient film temperature, i.e. $0.5(\bar{T}_{wt}+T_0)$. Comparisons between the predicted variations of transient $\overline{Nu}_L$ distributions with values of q_{cs}'' and H/B and the present experimental data are also made, and are shown in Figs. 13 and 14, respectively. Overall, a satisfactory trend is found in the present study, although a larger deviation occurs for time $t \geqslant 30$ min. This deviation is due to the larger uncertainty caused by the very small temperature difference measurements after $t \geqslant 30$ min.

As compared with the transient q_c''/q_{cs}'' distribution for a smooth channel without a rectangular rib, which was presented by Perng [9], it is plausibly found that the decay of the transient q_c'' distribution is slower in the present experiments, because of the existence of the ribbed obstruction (Fig. 15).

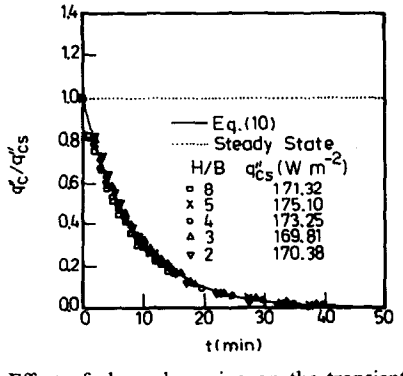

FIG. 12. Effect of channel spacing on the transient q_c''/q_{cs}'' distribution in the power-off period.

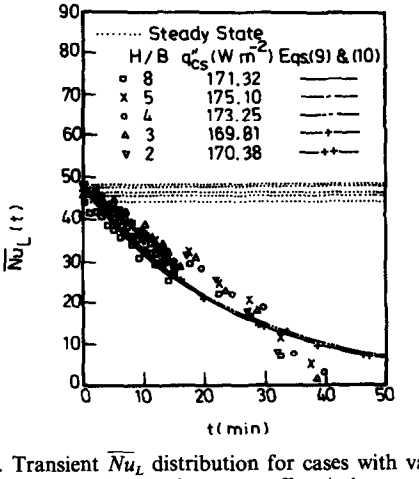

FIG. 14. Transient $\overline{Nu}_L$ distribution for cases with various H/B values in the power-off period.

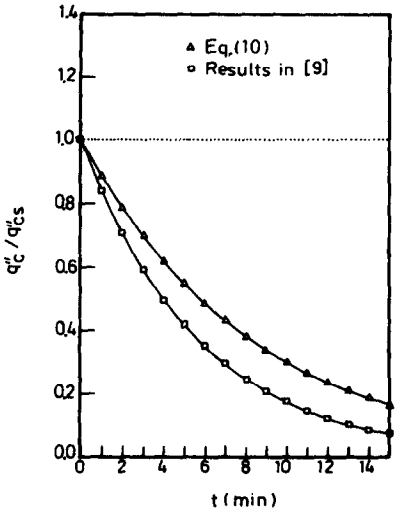

FIG. 15. Comparison of transient q''_c/q''_{cs} distributions between cases with and without a rib in the power-off period.

CONCLUSIONS

A series of systematic experiments for measuring transient natural convective heat fluxes in vertical parallel plates with a rectangular rib have been performed. Based on the present studies, the following conclusions may be drawn.

(1) A model to estimate transient heat distributions in the power-on and power-off periods—including the conductive heat loss, radiative heat loss, internal energy change of the test plate and convective heat transfer in the test channel—has been established.

(2) Two generalized correlations for estimating transient convective heat flux in both power-on and power-off periods are proposed. By using the proposed q''_c distributions, satisfactory agreements are achieved between the transient $\overline{Nu}_L$ predictions and experimental data.

(3) As compared with the correlations proposed for the cases of smooth plates without a ribbed obstruction, reasonable trends of transient q''_c/q''_{cs} distributions with larger time constants are found in the present experiments.

REFERENCES

1. A. Bar-Cohen and W. M. Rohsenow, Thermally optimum arrays of cards and fins in natural convection, *IEEE Trans. Components, Hybrids, Manufacturing Tech.* **CHMT-6**(2), 154–158 (1983).
2. A. Bar-Cohen and W. M. Rohsenow, Thermally optimum spacing of vertical, natural convection cooled, parallel plates, *ASME J. Heat Transfer* **106**, 116–123 (1984).
3. W. M. Kays and M. E. Crawford, *Convective Heat Transfer*, 2nd Edn. McGraw-Hill, New York (1980).
4. Y. H Hung and S. W. Perng, An experimental study of local steady-state natural convection in a vertical channel heated on one side wall, 25th ASME Natl Heat Transfer Conf., Houston, Texas, HTD-Vol. 96, pp. 165–171 (July 1988).
5. Y. H. Hung and W. M. Shiau, Local steady-state natural convection heat transfer in vertical parallel plates with a two-dimensional rectangular rib, *Int. J. Heat Mass Transfer* **31**, 1279–1288 (1988).
6. W. M. Shiau, Transient/steady-state experiments of natural convection heat transfer in vertical parallel plates with a two-dimensional rectangular rib, Master's Thesis, National Tsing Hua University, Taiwan (1987).
7. R. Seigel and J. R. Howell, *Thermal Radiation Heat Transfer*, 2nd Edn. McGraw-Hill, New York (1980).
8. S. J. Kline and F. A. McClintock, Analysis of uncertainty in single-sample experiments, *Mech. Engng* 3–8 (January 1953).
9. S. W. Perng, Experimental studies of transient/steady-state natural and forced convections in vertical parallel plates with asymmetric isoflux heating, Master's Thesis, National Tsing Hua University, Taiwan (1987).

UN MODELE EFFICACE POUR MESURER LE FLUX THERMIQUE EN CONVECTION NATURELLE VARIABLE ENTRE DES PLAQUES PARALLELES VERTICALES AVEC UN RUBAN RECTANGULAIRE

Résumé—Le transfert total de chaleur par convection naturelle variable dans des plaques parallèles verticales résulte de quatre mécanismes de transfert: pertes radiatives, pertes conductives, capacité thermique de la plaque de mesure et transfert convectif dans le fluide. A partir de ce modèle pour mesurer les distributions variables du transfert, on définit un flux thermique convectif variable sans dimension et on propose deux formules générales du flux thermique convection variable pour les périodes de stockage et de déstockage. De plus, en utilisant les distributions obtenues avec des formules, on estime correctement les nombres de Nusselt moyens dans chaque période de régime variable. Des comparaisons sont faites entre les calculs du $\overline{Nu}_L$ variable et les données expérimentales.

EIN MODELL ZUR MESSUNG DES INSTATIONÄREN WÄRMESTROMS BEI NATÜRLICHER KONVEKTION ZWISCHEN SENKRECHTEN PARALLELEN PLATTEN MIT EINER RECHTECKRIPPE

Zusammenfassung—Die Wärmeleistung, die bei einem Experiment zur Untersuchung der instationären natürlichen Konvektion zwischen senkrechten parallelen Platten mit einer Rechteckrippe abgeführt wird, besteht aus vier Anteilen: Strahlungsverluste, Leitungsverluste, in der Anordnung gespeicherter Wärme und schließlich der konvektiven Wärmeabgabe im Kanal. Für diese Anordnung zur Messung der instationären Wärmeverteilung wird ein dimensionsloser instationärer konvektiver Wärmestrom definiert. Dazu werden zwei allgemeine Gleichungen für den instationären konvektiven Wärmestrom vorgeschlagen, eine für den Zeitraum mit eingeschalteter Heizung und eine für die Zeit ohne Heizung. Zusätzlich werden mit Hilfe der zeitabhängigen Wärmeleistung und den vorgeschlagen Nusselt-Zahlen zeitliche Mittelwerte der Nusselt-Zahl während der Zeiträume mit und ohne Heizung erfolgreich abgeschätzt. Der Vergleich zwischen gemessenen und berechneten instationären Nusselt-Zahlen liefert eine befriedigende Übereinstimmung.

ЭФФЕКТИВНАЯ МОДЕЛЬ ДЛЯ ИЗМЕРЕНИЯ НЕСТАЦИОНАРНОГО ЕСТЕСТВЕННОКОНВЕКТИВНОГО ПОТОКА ТЕПЛА В ВЕРТИКАЛЬНЫХ ПАРАЛЛЕЛЬНЫХ ПЛАСТИНАХ С ПРЯМОУГОЛЬНЫМ РЕБРОМ

Аннотация—Суммарная теплота, подводимая в экзпериментах по исследованию нестационарной естественной конвекции в вертикальных параллельных пластинах с прямоугольным ребром, включает четыре вида потерь тепла: радиационные, кондуктивные, теплоемкость исследуемой пластины и конвективный теплоперенос в экспериментальном канале. На основе данной модели для измерения нестационарных распределений теплоты определяется безразмерный нестационарный конвективный тепловой поток и предлагаются два обобщенных соотношения для этого потока в случаях переходных периодов в процессах включения или выключения подогрева. Кроме того, используя полученные распределения q_c'' и предложенные корреляции для числа Nu, успешно оцениваются переходные средние числа Нуссельта в переходных режимах при включении или при выключении подогрева. Сравнение расчетов переходного числа $\overline{Nu}_L$ с экспериментальными данными дало удовлетворительный результат.